Electrostatic Effect upon Association of Reduced Nicotinamide Adenine Dinucleotide and Equine Liver Alcohol Dehydrogenase†

Chris R. Lively, Benjamin A. Feinberg, and James T. McFarland*

Department of Chemistry and Laboratory for Molecular Biomedical Research, The University of Wisconsin—Milwaukee, Milwaukee, Wisconsin 53201

Received November 13, 1986; Revised Manuscript Received April 29, 1987

ABSTRACT: The rate of association of equine liver alcohol dehydrogenase and its coenzymes exhibits a large pH dependence with slower rates at basic pH and an observed kinetic pK_a value of approximately 9–9.5. This pH dependence has been explained by invoking local active site electrostatic effects which result in repulsion of the negatively charged coenzyme and the ionized hydroxyl anion form of the zinc-bound water molecule. We have examined a simpler hypothesis, namely, that the pH dependence results from the electrostatic interaction of the coenzyme and the enzyme which changes from an attractive interaction of the negatively charged coenzyme and the positively charged enzyme to a repulsive interaction between the two negatively charged species at the isoelectric point for the enzyme (pH 8.7). We have tested this proposal by examining the ionic strength dependence of the association rate constant at various pH values. These data have been interpreted by using the Wherland–Gray equation, which we have shown can be applied to the kinetics of enzyme–coenzyme association. Our results indicate that the shielding of the buffer electrolyte changes from a negative to a positive value as the charge on the protein changes at the isoelectric point. This result is exactly that which is predicted for electrostatic effects that depend on the charge of the protein molecule and is not consistent with predictions based upon the local active site effects. At low ionic strength values of 10 mM or less, approximately 75% of the observed pH dependence results from the enzyme electrostatic effects; the remaining pH dependence may result from active site effects. This result emphasizes the necessity of correcting bimolecular rate constants of enzyme reactions for electrostatic effects.

The association of NADH[1] and LADH is a single-step kinetic process at 10–25 °C. The rate of this process can be followed analytically from the increase in fluorescence of NADH as the stacking of nicotinamide and adenine is disrupted upon enzyme binding or from the decrease in fluorescence of the protein during coenzyme binding (DeTraglia et al., 1977). The ratio of the forward and reverse rate constants is approximately equal to the equilibrium constant for the binding of NADH, indicating that the reaction consists of a single step as previously suggested (Geraci & Gibson, 1967). It should be noted that equality between the ratio of forward and reverse rate constants and the equilibrium constant is also expected for a two-step reaction in which the second kinetic step in the forward direction is much larger than its reverse.

There is a large pH dependence of the association rate constant with rapid binding at acidic pH values and decreasing rate constants below pH 8; the observed pK_a value for this process is 9.0–9.5 (DeTraglia et al., 1977; Oldén & Pettersson, 1982). Anions slow the rate of binding of nucleotide, and the pH dependence completely disappears at high anion concentration (Oldén & Pettersson, 1982).

It has been suggested that the pH dependence of nucleotide association is caused by the local active site electrostatic effect from the ionization of the zinc-bound water molecule. In this model there is electrostatic repulsion between the hydroxide form of the enzyme and the negatively charged pyrophosphate of NADH, resulting in slower reaction rates (Andersson et al., 1984). The repulsion results from the change in charge of the active site from 0 to −1 upon ionization of the zinc-bound water molecule. The anion effect could result from anion binding to the active site zinc (Andersson et al., 1984) and/or from the competition of anion and NADH for the anion binding site (arginine-47) at which the NADH pyrophosphate normally binds (Oldén & Pettersson, 1982; Andersson et al., 1984). These simple active sites models for the effect of anion and pH dependence of NADH and LADH are not supported by the observation that the apo-zinc enzyme shows the same pH dependence of nucleotide binding as the native enzyme (Dietrich et al., 1983). It has been suggested, however, that fortuitous equivalence between the pK_a of zinc-bound water and the zinc ligands, cysteines-46 and -174, in the apo-zinc enzyme could result in the observation of similar pH dependences for the native and apo-zinc enzymes (Andersson et al., 1984).

We have carried out an experimental test of a simpler hypothesis for the pH and anion dependence of the nucleotide rate constant, namely, that both result from the electrostatic effect of the charge on the protein and nucleotide and the shielding of this effect by added electrolyte. The experimental isoelectric point for LADH (8.7) is in the region of the observed pK_a (Lutstorf et al., 1970), and the predicted charge of the enzyme, Table I, changes from positive to negative at pH 8.6 at 25 °C and pH 8.8 at 10 °C, values near the observed kinetic pK_a and isoelectric point. It is, therefore, possible that the decrease in rate of nucleotide binding occurs as the result of a change in electrostatic effect from an attractive effect of

† This research was supported by Grant GM32504 from the National Institutes of Health.

* Address correspondence to this author at the Department of Chemistry, University of Wisconsin—Milwaukee.

[1] Abbreviations: LADH, equine liver alcohol dehydrogenase; NADH, nicotinamide adenine dinucleotide; DTT, 1,4-dithiothreitol; Cys, cysteine; His, histidine; Lys, lysine; Arg, arginine; Ser, serine.

0006-2960/87/0426-5719$01.50/0

the positively charged protein and the negatively charged nucleotide at pH values below pH 8.7 to the repulsive effect between the negatively charged protein and nucleotide at pH values above 8.7. Such effects have been widely studied in electron-transfer proteins (Wherland & Gray, 1981; Feinberg & Ryan, 1981). Electrostatic effects upon the rate of association of LADH and NADH would result in faster rates of association for oppositely charged species with the observed rates increasing with increased positive charge upon the protein. Correspondingly, repulsive effects between species of the same charge would result in increasingly slower rates as the negative charge on the protein increases. Furthermore, the anion effect outlined previously could result from the electrolyte shielding of the electrostatic forces. This shielding would be expected to increase with increasing ionic strength, reaching an asymptote at high electrolyte concentration. Since electrolyte simply shields the electrostatic forces, added electrolyte would be expected to slow the rate of reaction between species of opposite charge and to stimulate the rate of reaction between species of like charge. At pH values below 8.7, added electrolyte would be expected to slow the rate of NADH binding to enzyme by shielding the attractive interaction. The effect of electrolyte should change from inhibitory to stimulatory at pH values above 8.7 as the charge on the protein becomes negative and added electrolyte would shield the repulsion. Accordingly, we report the change in the electrolyte shielding of the rate constant for the association of NADH and LADH as a function of pH.

Experimental Procedures

Reagents. LADH was a crystalline suspension obtained from CalBiochem (lot no. 903808). NADH was PL–Pharmacia "Chromata-pure" and was used without further purification. Sodium phosphate (MCB), 1,4-dithiothreitol (Sigma), and pyrazole (Aldrich Chemical Co.) were used without further purification. Concentration of protein solutions was achieved with a Schleicher & Schuell collodion bag protein concentrator (Model UH 100/2, with UH 100/25 collodion bags). Single-wavelength absorbance determinations were made with a Cary 16 spectrophotometer. The conductivity of the buffer solutions was determined with a radiometer/Copenhagen conductivity meter CDM3. A Corning pH meter Model 130 was used for all pH determinations.

Enzyme Preparation and Activity Determination. The enzyme was supplied as a crystalline suspension in 10% ethanol solution. The ethanol was removed by decantation after low-speed centrifugation of the suspension. The solid was resuspended in 5 mM phosphate buffer (pH 8.0) and incubated for 18–24 h with a 2:1 excess of 1,4-dithiothreitol (DTT). The precipitate was chromatographed on a Bio-Gel P-30 column in order to separate the enzyme from DTT and any residual ethanol. During chromatography, the enzyme peak was detected by its 280-nm absorbance (ϵ_{280nm} = 35 300 M^{-1} cm^{-1}). The enzyme active site concentration was determined by titration with NAD^+–pyrazole (Theorell & Yonetoni, 1963) (difference extinction coefficient, $\Delta\epsilon_{300nm}$ = 7220 N^{-1} cm^{-1}), and the fraction of sites that are active was determined from the comparison between this active site concentration and the enzyme concentration determined from its extinction coefficient. In these experiments the fractional activity of LADH was always >90%; the concentration of LADH is given as the normality of active site monomers within the dimeric enzyme.

Buffer Preparation. Buffers were 5 mM phosphate. They were prepared by mixing 5 mM solutions of mono-, di-, and tribasic sodium phosphate in the appropriate proportions to achieve the desired pH; the ionic strength of these solutions was adjusted to the desired value by the addition of sodium chloride. The conductivity and pH of the buffer solutions were measured before and after the experiments to assure that the ionic strength of the solutions remained constant after preparation.

Coenzyme Preparation. Solutions of varying concentrations of NADH at the different pH and ionic strength values were prepared the day of the experiment. The concentrations were determined by spectrophotometric readings at 340 nm (ϵ_{340nm} = 6220 M^{-1} cm^{-1}) just prior to use. Since NADH is unstable at alkaline pH values, coenzyme solutions were made basic just before introduction into the stopped-flow spectrometer.

Stopped-Flow Kinetic Experiment. Kinetic data were obtained on a Durrum stopped-flow spectrofluorometer with a pneumatic air-actuated pushing device to drive the two syringes, one containing LADH and the other NADH. Enzyme fluorescence changes were monitored with the use of a xenon arc lamp excitation source and a monochrometer set at a wavelength of 280 nm for fluorescence excitation of LADH; emission was measured through a Corning 0-54 filter (cutoff <300 nm) by a photomultiplier tube (PMT) positioned at 90° to the incident light. The PMT voltages were measured with a rapid A–D converter interfaced to an IBM PC. The kinetic traces were saved on floppy disk and treated by regression analysis utilizing the pseudo-first-order rate law; pseudo-first-order conditions (NADH concentrations greater than 5 times LADH concentrations) were maintained throughout all stopped-flow experiments. The stopped-flow mixing chamber has a dead time of 3 ms, making determinations of rate constants greater than 250 s^{-1} difficult. For this reason, we ran experiments at 10 °C to slow the reaction rates; this permitted more accurate determination of rate data at low pH and ionic strength values.

Determination of the Rate Constant for Association of LADH and NADH. Kinetic experiments were run under pseudo-first-order conditions. The association of LADH and NADH was followed by the decrease in enzyme fluorescence (280-nm excitation) upon binding NADH. The determination of rate constant from the increase in NADH fluorescence caused by unstacking of the bases during binding to the enzyme gave equivalent results. Figure 1 shows a typical kinetic trace of the LADH fluorescence quenching resulting from NADH binding. Analysis of this curve by the first-order rate expression results in a value of k_{obsd} for a series of NADH concentrations. The following equation relates these values of k_{obsd} to the rate constants for association and dissociation of LADH–NADH:

$$k_{obsd} = k_1[\text{NADH}] + k_{-1}$$

A plot of k_{obsd} vs. [NADH] has a slope equal to the association rate constant k_1 and an intercept equal to the dissociation rate constant k_{-1}. The slope of this plot was calculated by linear least-squares regression on an IBM PC. The fluorescence method we have employed does not give sufficiently accurate results to allow satisfactory determination of the intercept to give a reliable value of k_{-1}.

Calculations. The calculations leading to the data analysis and predictions shown in the figures and tables were carried out as follows: The first step was the calculation of the change on LADH as a function of pH; this was evaluated from determination of the best fit values from the application of the Wherland–Gray equation (Wherland & Gray, 1976) to the data that we collected from the pH and ionic strength dependence of the rate constant for association of LADH and NADH. The statistical method that we chose to use was the Monte Carlo random walk technique (Schreider, 1966) for

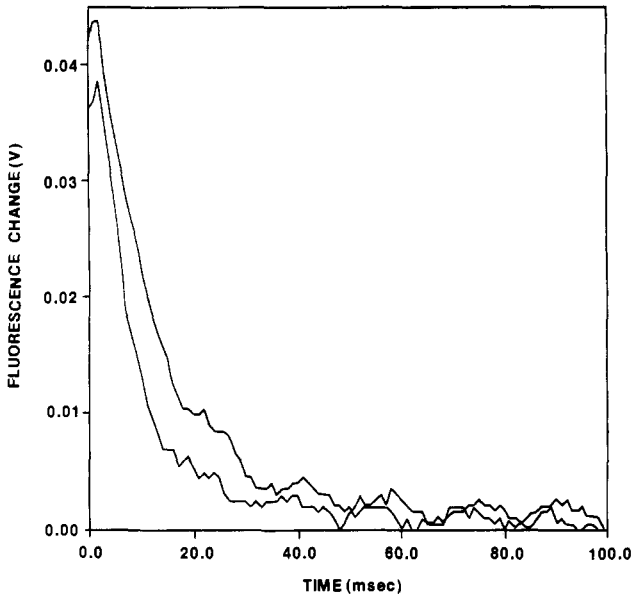

FIGURE 1: Kinetic profile for the reaction of LADH–NADH. The reaction kinetics are followed from the time dependence of the decrease in fluorescence of LADH as NADH binds. λ_{ex} = 280 nm, λ_{em} > 320 nm, [LADH] = 3 μN, 5 mM phosphate buffer, pH 7.0, 10 °C. Upper trace, [NADH] = 20.1 μM, 100 mM NaCl; lower trace, [NADH] = 17.8 μM.

the variation of the charge of LADH and the value of k_∞. The parameters for charge on NADH (−2) and radii for LADH (55 Å) and NADH (7.0 Å) were assigned fixed values. The latter values are the largest elliptical radii from X-ray studies (Brändén et al., 1975; Banaszak & Webb, 1975). The best fit values for the LADH charge were determined by minimizing the square of the residuals between experimental and calculated data. Figure 2 shows the best fit plot superimposed upon the experimental data, and Table I shows the resultant values of the LADH charge as a function of pH along with values calculated from the amino acid sequence as outlined below.

In order to see if the observations were consistent with the behavior expected for the electrostatic effects predicted for the whole protein or the local active site electrostatic effect of the zinc-bound water molecule, we needed to evaluate the charge upon the LADH molecule with the exclusion of the amino acid residues whose acid–base properties are affected by zinc ligation. For the purposes of this calculation, we excluded the two cysteine ligands (Cys-46 and Cys-174), the histidine ligand (His-67), the zinc-bound water molecule, and the zinc itself. In addition, we removed four cysteine residues bound to the structural zinc since these are not ionizable. All of the residues listed above were excluded from the calculation of LADH charge as a function of pH. For the equivalent calculation of the charge of the active site zinc bound water, we assigned the pK_a value of 9.3 to this water molecule; this value is the pK_a observed for the pH dependence of NADH association (DeTraglia et al., 1977; Oldén & Pettersson, 1982). Both calculations involve substitution of the appropriate charges into the Wherland–Gray equation. For the protein as a whole these were obtained from the amino acid composition and typical pK_a values (Tanford & Hauenstein, 1956) of these amino acid residues in proteins. These calculations are reported at 10 °C because experiments were carried out at 10 °C rather than 25 °C. The low-temperature calculations were the result of extrapolation of the pK_a values using the van't Hoff equation and values of reaction enthalpy for amino acid ionization (*CRC Handbook of Biochemistry*, 1970).

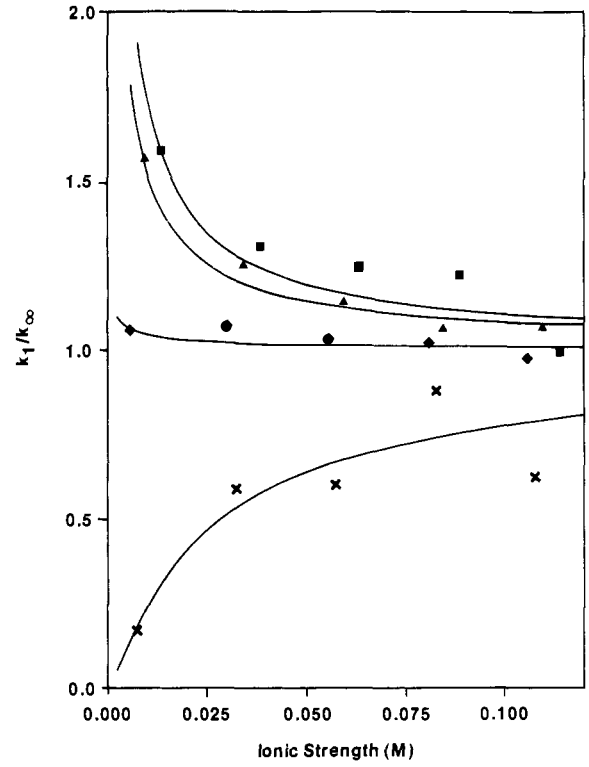

FIGURE 2: Ionic strength dependence of the NADH–LADH association rate constant. k_1 is derived from the slope of a plot of the pseudo-first-order rate constant from Figure 1 against NADH concentration. The buffers used in this experiment were all 5 mM phosphate buffers with NaCl added as an ionic strength buffer; all experiments were carried out at 10 °C. The solid lines are the best fit plots from the Wherland–Gray equation. The pH values were (■) 7.0, (▲) 8.0, (♦) 9.0, and (×) 10.0.

Figures 3 and 4 show the predictions of electrostatic behavior as a function of pH and ionic strength for the model involving the charge on the protein while Figures 5–8 show equivalent calculations for the local active site electrostatic effects.

RESULTS

Figure 1 shows the single-exponential complexation of NADH and LADH in the presence and absence of added electrolyte. The electrolyte concentration of the buffer solutions was evaluated in terms of the ionic strength of the solution; this was adjusted to the desired value with NaCl. At pH 7.0 the rate constant decreases at higher ionic strength (Figure 1). Figure 2 shows the ionic strength dependence of the NADH–LADH association rate constant at pH 7.0, 8.0, 9.0, and 10.0. Notice that the slope of the plot of rate constant vs. ionic strength is negative at pH 7.0 and 8.0 and that at pH 9.0 there is almost no dependence upon ionic strength. At pH 10.0 there is an ionic strength dependence in the opposite direction to that at the more acidic pH values. These data are consistent with electrolyte shielding of an attractive electrostatic interaction between negatively charged NADH and positively charged protein at pH values of 7.0 and 8.0, with a small electrostatic effect at pH 9.0, and with electrolyte shielding of the electrostatic repulsion between negatively charged NADH and negatively charged protein at pH 10.0.

Table I shows the parameters derived from fitting our data to the Wherland–Gray equation for electrostatic rate effects. This equation was derived to describe the electrostatic effect in outer-sphere electron-transfer reactions and is based upon Marcus theory, which models such processes. However, the following considerations show that the Wherland–Gray equation also applies to a bimolecular association process. For

Table I: Comparison of Observation and Calculation Based upon Models

pH	$k_\infty \times 10^{-6}$ (s^{-1} m^{-1})	LADH charge, W–G[a] fit of data	LADH charge from sequence, 10 °C	pH value at which W–G[a] fit and sequence are equivalent	LADH charge at active site zinc bound water	LADH charge at active site His-51 or Lys-228
7	3.1	11.75	15.8	7.4	−0.005	0.994
8	2.3	8.57	7.4	7.8	−0.047	0.941
9	2.1	0.93	−2.8	8.7	−0.33	0.613
10	1.4	−27.67	−23.8	10.1	−0.84	0.137

[a] W–G, Wherland–Gray.

a reaction such as association of NADH and LADH, transition-state rate theory gives the expression:

$$k = \frac{kT}{h} e^{-\Delta G^*/RT} \quad (1)$$

Substituting for ΔG^* in eq 1:

$$\Delta G^* = \Delta G^* + W$$

where ΔG^* is the transition-state free energy, ΔG^* is the transition-state free energy independent of the electrostatic effect, and W is the electrostatic potential energy term, leading to the expression:

$$\ln k = \ln k^* - W/RT$$

Letting $k^* = k_\infty$, the rate constant at infinite ionic strength, i.e., the rate constant that is independent of any electrostatic energy term, we obtain

$$\ln k = \ln k_\infty - W/RT \quad (2)$$

The electrostatic potential between charged species in solution has been described previously (Alberty & Hammes, 1958):

$$W = \frac{1}{2}\left(\frac{e^{\kappa R_1}}{1+\kappa R_1} + \frac{e^{\kappa R_2}}{1+\kappa R_2}\right)\left(\frac{Z_1 Z_2 e^2}{\epsilon}\right)\left[\frac{e^{-\kappa(R_1+R_2)}}{R_1+R_2}\right]$$

Substitution of W in eq 2 followed by simplification leads to an expression identical with the Wherland–Gray equation:

$$\ln k = \ln k_\infty - A\left(\frac{e^{-\kappa R_1}}{1+\kappa R_2} + \frac{e^{-\kappa R_2}}{1+\kappa R_1}\right)\left(\frac{Z_1 Z_2}{R_1+R_2}\right) \quad (3)$$

$$A = 3.576 \text{ at } 25\ ^\circ\text{C} \qquad A = 3.799 \text{ at } 10\ ^\circ\text{C}$$

The parameters we have used in these calculations are the protein radius from the X-ray data for LADH (Brändén et al., 1975) (we have used the larger ellipsoidal dimension for the dimer), the radius of NADH from X-ray crystal data (Banaszak & Webb, 1975) (again the larger ellipsoidal radius), and the charge of −2 throughout the pH range for NADH. We have varied ln k_∞ and the charge on the protein using Monte Carlo methods until the best fit as evaluated by the minimum residual between our measurements and the calculations was achieved. The parameters representing the charge on LADH and the rate constant at infinite ionic strength shown in Table I are these "best fit" values.

Table I also shows the net charge of the protein at each of the four pH values investigated; the fourth column shows the values calculated from the amino acid content of the protein dimer with the exception of the active site zinc ligands and the cysteine residues bound to the structural zinc atom. The sixth column shows the equivalent calculations for the zinc bound water molecule at the active site, and the seventh column shows the calculation for His-51 and Lys-228. Notice that agreement between the protein charge as a function of pH evaluated from the Wherland–Gray treatment of our data,

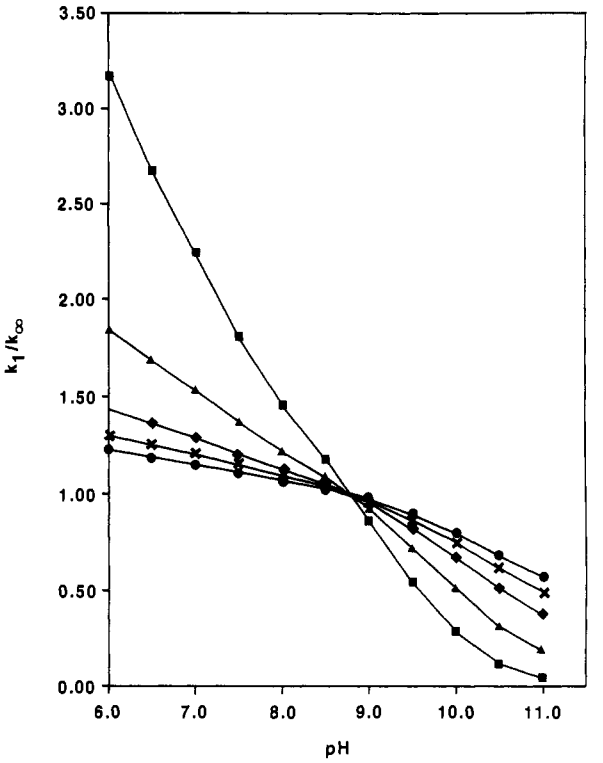

FIGURE 3: Calculation of the pH dependence of the rate constant for LADH–NADH association at several values of ionic strength based on the whole protein. Parameters used in the Wherland–Gray equation were R_{NADH} = 7 Å, R_{LADH} = 55 Å, Z_{NADH} = −2, and Z_{LADH} = charge calculated from sequence data as described under Experimental Procedures. The ionic strength values were (■) 10, (▲) 25, (♦) 50, (×) 75, and (●) 100 mM.

Table I, and the calculated charge on the protein is quite good. It appears that the two differ by no more than 0.4 pH unit. The data in Figure 2 and Table I are consistent with assignment of most of the pH dependence of nucleotide binding to electrostatic effects; however, the rate constant at infinite ionic strength changes by a factor of 2.2 over the pH range studied. Thus, about 85% of the pH dependence can be attributed to the electrostatic effects at an ionic strength of 5.0 mM. This percentage of the total pH dependence falls to 75% at 10 mM and to 40% at 100 mM.

Discussion

Figures 3 and 4 show the pH and ionic strength dependence of the rate constant for association of NADH and LADH; these were calculated by using the Wheland–Gray equation and the charge on the protein determined from the amino acid composition of LADH with the amino acid residues that are ligated to zinc excluded. The radii of LADH and NADH were evaluated as described previously, and the charge of NADH was assigned as −2 throughout the pH range. Figure 3 shows a plot of the pH dependence of the rate constant at various values of ionic strength. Oldén and Pettersson have shown the effect of anionic buffer at two different salt concentrations;

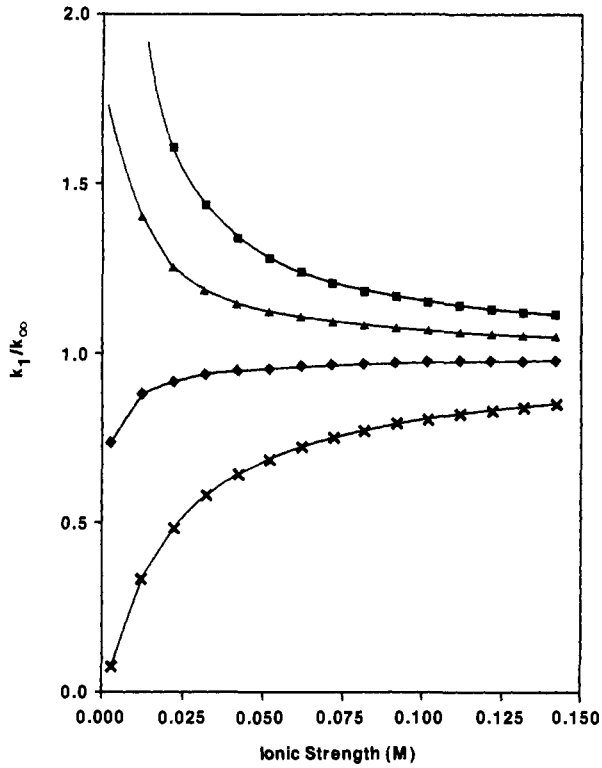

FIGURE 4: Calculation of the ionic strength dependence of the rate constant for LADH–NADH association at several pH values based on the whole protein. Parameters used in the Wherland–Gray equation were those shown with Figure 3. The pH values were (■) 7.0, (▲) 8.0, (♦) 9.0, and (×) 10.0.

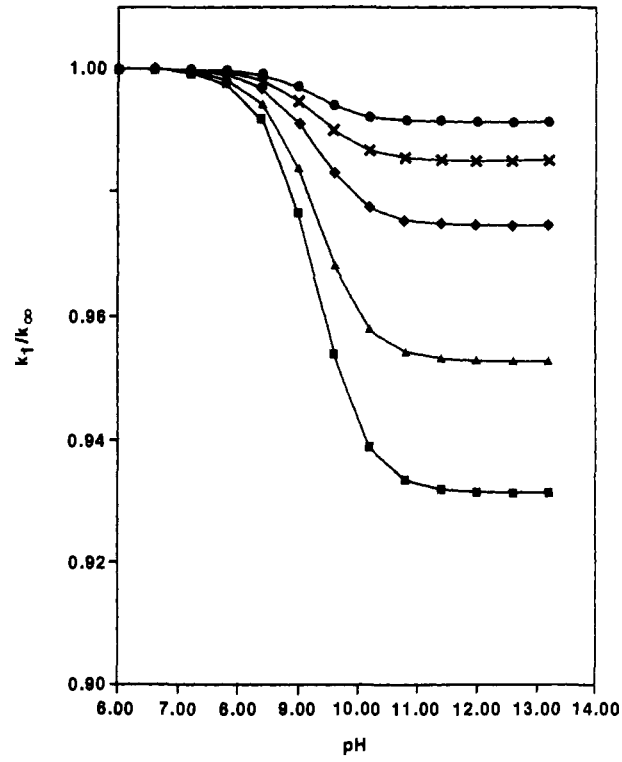

FIGURE 5: Calculation of the pH dependence of the rate constant for LADH–NADH association at several values of ionic strength based on the active site zinc bound water ionization. Parameters used in the Wherland–Gray equation were R_{NADH} = 7 Å, R_{LADH} = 55 Å, Z_{NADH} = −2, and Z_{LADH} = 0 above the LADH–NADH association pK_a or −1 below this pK_a. The ionic strength values were (■) 5, (▲) 10, (♦) 25, (×) 50, and (●) 100 mM.

the correspondence between the predicted electrostatic behavior and the observations of Oldén and Pettersson is striking. There are two major differences between the calculated and observed values: (1) the absence of a clear asymptote for the pH–rate profile at low pH values and (2) the value of the asymptote for the rate vs. pH plot at high ionic strength and high pH values.

The first discrepancy may result from a change in the rate-limiting step as a function of pH since the pH–rate profile of NADH association reaches an asymptote at pH 7 and then decreases at pH 6 (DeTraglia et al., 1977). We examined the possibility that the lack of a clear asymptote at low pH resulted from the fact that the electrostatic effect results only from the residues on the same face of the protein as the NADH binding site. To examine this possibility, we calculated the pH dependence of the association rate constant using the Wherland–Gray equation and the charge on that part of the protein on the same side of the enzyme molecule as the NADH binding site. This calculation does not satisfactorily fit the data. The calculated pK_a value for the kinetics of NADH association is much more acidic (6.8) than predicted on the basis of the whole protein charge and is much more acidic than the observed value. Furthermore, the charge at low pH values is much smaller than that calculated from the experimental data. Thus, this model for involvement of only part of the protein in the electrostatic effect does not seem warranted.

The second discrepancy may be explained as follows. The electrostatic treatment predicts that the plot should show an asymptote for the rate constant near zero at low ionic strength but a value above zero at high ionic strength. The latter prediction is the result of electrolyte shielding of the repulsive interaction between negatively charged enzyme and negatively charged coenzyme. The observed data show the expected behavior at pH values below 8.8, but the rates above that pH are lower than predicted. This behavior may be the result of superimposed inhibition resulting from anion binding to the pyrophosphate binding site. Thus, only part of the anion effect upon the association of NADH and LADH is electrostatic; the remainder is a pH-independent inhibition. It is clear from the comparison of the calculated and observed data that the electrostatic model which takes account of the charge on the protein and coenzyme is capable of providing an adequate explanation for most of the pH dependence and the anion effect upon the pH dependence observed by our group and others. As explained earlier, the electrostatic effect is not the only factor determining the pH dependence of this reaction, but at moderate to low ionic strength, it is the dominant effect.

Figure 4 shows a calculation of the pH dependence of the ionic strength effect based upon amino acid composition. This calculation can be compared directly to the experimental data in Figure 2. The qualitative agreement is very good; as can be seen in Table I, the quantitative agreement between the LADH charge calculated from the Wherland–Gray equation applied to our pH and ionic strength data is also quite good with charges calculated from the Wherland–Gray equation within 0.4 pH unit of the values of charge on the protein dimer calculated from the amino acid composition. The only significant difference between experimental data and calculation is that the asymptote of the ionic strength plot is not pH independent, indicating that there is a small (2.2-fold) pH effect independent of the electrostatic effect.

Figures 5 and 6 show a calculation of the pH and ionic strength dependence of the NADH–LADH association rate constant based upon the Wherland–Gray equation, but taking into account only the electrostatic effect of the active site zinc bound water ionization. For this model, the charge at the active site of LADH is nearly zero at pH values less than 9.3 and −1 at pH values above 9.3. Therefore, there would be no

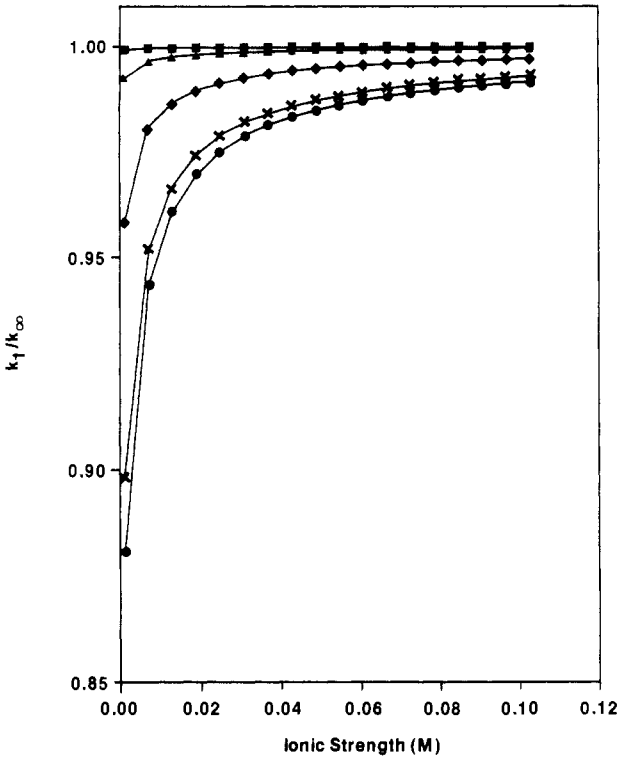

FIGURE 6: Calculation of the ionic strength dependence of the rate constant for LADH–NADH association at several pH values based on the active site zinc bound water ionization. Parameters used in the Wherland–Gray equation were those shown with Figure 5. The pH values were (■) 7.0, (▲) 8.0, (♦) 9.0, (×) 10.0, and (●) 11.0.

Chart I

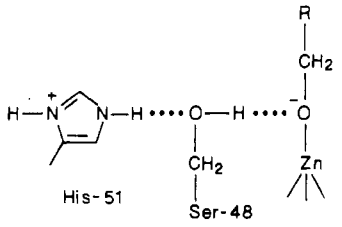

electrolyte shielding effect below pH 9.3 and a stimulation of rate at high ionic strength above that pH (Figure 5); there would be no gradual change in electrolyte shielding since the active site pH transition would not show a continual change in charge as the enzyme does. Thus, this model would adequately explain our observations only at pH 9 and 10 but not at pH values of 7 and 8. Figure 6 shows the predicted pH dependence of the rate constant at various ionic strength values. This active site electrostatic effect does not, as previously stated (Andersson et al., 1984), predict the observed behavior. The effect of added electrolyte can only increase the rate constant for the reaction by shielding the repulsive force between the two negatively charged species whereas the experimental data of Oldén and Pettersson show a decrease in rate constant with added electrolyte. The poor correspondence between this electrostatic interaction including only active site zinc bound water molecule and the measured pH dependence indicates that explanations based only on the active site electrostatic considerations resulting from ionization of the zinc-bound water molecule are inadequate to explain the experimental data. It is possible that the ionic equilibrium that determines the rate of nucleotide binding is not associated with the ionization of zinc-bound water and originates from other active site residues. The acid–base catalytic unit at the active site of LADH consists of two amino acid groups and the zinc-

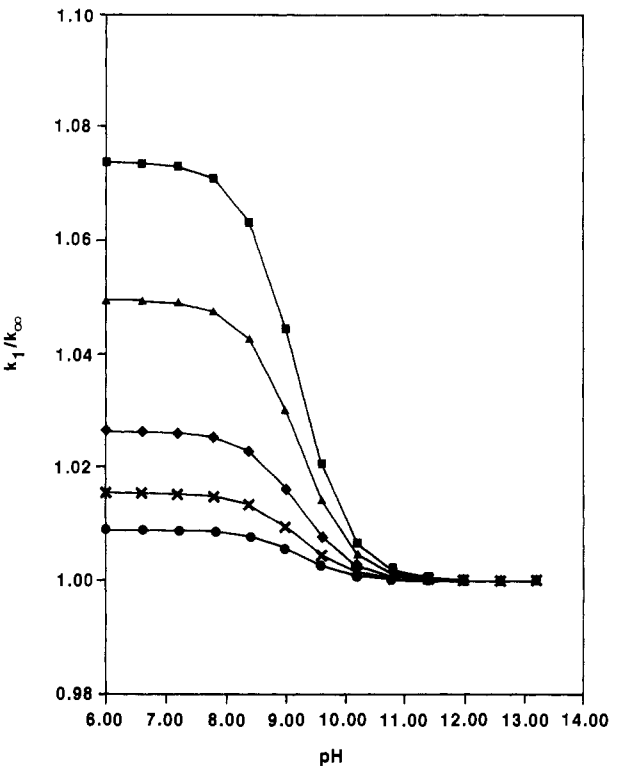

FIGURE 7: Calculation of the pH dependence of the rate constant for LADH–NADH association at several values of ionic strength based on the active site ionization of His-51 or Lys-228. Parameters used in the Wherland–Gray equation were R_{NADH} = 7 Å, R_{LADH} = 55 Å, Z_{NADH} = −2, and Z_{LADH} = 1 above the LADH–NADH associtaion pK_a or 0 below this pK_a. The ionic strength values were (■) 5, (▲) 10, (♦) 25, (×) 50, and (●) 100 mM.

bound water molecule; Chart I shows a catalytic triad of these active site groups that contribute to the base-catalyzed removal of the proton from alcohol being oxidized in the LADH-catalyzed reaction. It has been suggested that the pK_a of this triad is controlled by ionization of the His-51 (Cook & Cleland, 1981). This assignment is consistent with the fact that removal of the active site zinc does not result in the loss of pH dependence of nucleotide association (Dietrich et al., 1983) or of a similar pK_a observed in the fluorescence spectrum of LADH (Eftink, 1986). It is also consistent with the observation that metal substitution does not perturb the first pK_a = 6.5 observed in the dependence of k_{cat}/K_m (Makinen et al., 1983). Furthermore, mutagenesis studies indicate that His-51 is responsible for the ionization equilibrium that determines the pH dependence of k_{cat} and k_{cat}/K_m (Plapp et al., 1986). If the pK_a of His-51 controls the base-catalyzed removal of the substrate proton during catalysis, the pK_a value of 9.3 which controls nucleotide association might also be the result of His-51 ionization. This would lead to a mechanism in which the positively charged triad would control binding of NAD^+ which in turn would perturb the pK_a to 7.5, resulting in the production of the catalytically active neutral form of the triad at basic pH values. In light of these considerations, we have modeled the active site electrostatic interactions with NADH using the ionization of His-51 and a change in active site charge of +1 − 0; the calculated pH and ionic strength dependencies are shown in Figures 7 and 8 and Table I. It is clear that this localized active electrostatic effect as described does not account for the data since the effect of anion is inhibitory across the entire pH profile and the magnitude of the ionic strength effect is too small. Finally, we have examined a third active site electrostatic model involving Lys-228; we feel this is a likely group near the active site which could

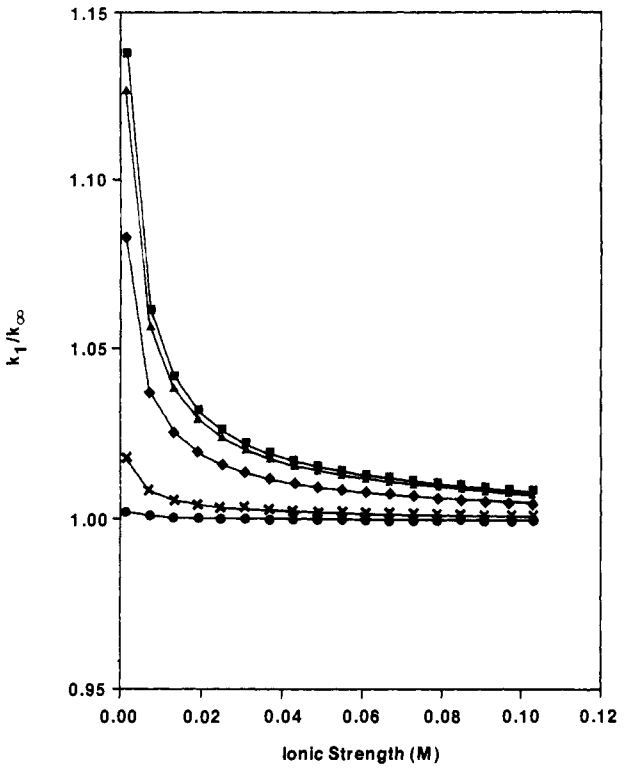

FIGURE 8: Calculation of the ionic strength dependence of the rate constant for LADH–NADH association at several pH values based on the active site ionization of His-51 or Lys-228. Parameters used in the Wherland–Gray equation were those shown in Figure 7. The pH values were (■) 7.0, (▲) 8.0, (♦) 9.0, (×) 10.0, and (●) 11.0.

control the pH dependence of nucleotide binding. Since the charge for this electrostatic model would change from +1 to 0 with the observed nucleotide association pK_a of 9.3, our prediction is identical with the model describing the ionization of His-51. In summary, none of the active site electrostatic models are consistent with the experimental data since all fail to predict both the direction and magnitude of the effect of buffer electrolyte upon nucleotide association rates. It is not clear at present which group(s) at the active site may contribute to the residual pH dependence observed at infinite ionic strength.

Our observations are also inconsistent with other models for the effect of added electrolytes upon the coenzyme association reaction. Anion binding to Arg-47 of the nucleotide binding site (Andersson et al., 1984) would result in competitive inhibition at all pH values with decreasing rates at higher electrolyte concentration. Formation of a zinc–anion complex would result in a negatively charged active site at all pH values and in the observation of a stimulation in rate with increasing electrolyte concentration regardless of pH. The experimental data we have presented in this paper are consistent with neither of these predictions, although it is clear that a part of the effect of anions upon the rate of NADH–LADH association is a competitive pH-independent inhibition. This inhibition most likely results from anion binding to Arg-47.

In summary, the pH dependence and electrolyte dependence of the rate constant for association of NADH–LADH are consistent with electrolyte shielding of the attraction or repulsion of negatively charged NADH by the positively or negatively charged protein. This investigation emphasizes the importance of correcting pH profiles of bimolecular enzyme kinetic processes for electrostatic effects before interpreting such data.

Registry No. ADH, 9031-72-5; NADH, 58-68-4.

REFERENCES

Alberty, R. A., & Hammes, G. G. (1958) *J. Phys. Chem. 62*, 154–159.

Andersson, P., Kvassman, J., Oldēn, B., & Pettersson, G. (1984) *Eur. J. Biochem. 138*, 603–609.

Banaszak, L. J., & Webb, L. E. (1975) *Structure and Conformation of Nucleic Acids and Protein–Nucleic Acid Interactions* (Sundaralingam, M., & Rao, S. T., Eds.) pp 375–386, University Park Press, Baltimore, MD.

Brändēn, C.-I., Jörnvall, H., Eklund, H., & Furgren, B. (1975) *Enzymes (3rd Ed.) 11*, 103–190.

Cook, P. F., & Cleland, W. W. (1981) *Biochemistry 20*, 1805–1816.

CRC Handbook of Biochemistry (1970) 2nd ed., pp J-58–J-153, CRC Press, Cleveland, OH.

DeTraglia, M. C., Schmidt, J., Dunn, M. F., & McFarland, J. T. (1977) *J. Biol. Chem. 252*, 3493–3500.

Dietrich, H., MacGibbon, A. K. H., Dunn, M. F., Zeppezauer, M. (1983) *Biochemistry 22*, 3432–3438.

Eftink, M. R. (1986) *Biochemistry 25*, 6620–6624.

Feinberg, B. A., & Ryan, M. D. (1981) *Top. Bioelectrochem. Bioenerg. 4*, 225–270.

Geraci, G., & Gibson, Q. H. (1967) *J. Biol. Chem. 242*, 4275–4278.

Lutstorf, U. M., Schurch, P. M., & von Wartburg, J. T. (1970) *Eur. J. Biochem. 17*, 497–508.

Makinen, M. (1983) *Proc. Natl. Acad. Sci. U.S.A. 80*, 2584–2588.

Oldēn, B., & Pettersson, G. (1982) *Eur. J. Biochem. 125*, 311–315.

Plapp, B. V., Gould, R. M., Green, D. W., Ganzhorn, A. J., & Hershey, A. D. (1986) *VIth Midwest Enzyme Chemistry Conference*, Loyola University, Chicago, IL (Abstract 11a).

Shreider, Yu. A. (1966) *The Monte Carlo Method*, Permagon Press, Oxford.

Tanford, C., & Hauenstein, J. D. (1956) *J. Am. Chem. Soc. 78*, 5287–5291.

Theorell, H., & Yonetani, T. (1963) *Biochem. Z. 338*, 537–553.

Wherland, S., & Gray, H. B. (1976) *Proc. Natl. Acad. Sci. U.S.A. 73*, 2950–2954.

Wherland, S., & Gray, H. B. (1981) *Biological Aspects of Inorganic Chemistry* (Addison, A. W., Cullen, W. R., Dolphin, D., & James, B. R., Eds.) pp 289–368, Wiley, New York.